THERMAL RADIATION EFFECTS ON MAGNETOHYDRODYNAMIC FLOW AND HEAT TRANSFER IN A CHANNEL WITH POROUS WALLS OF DIFFERENT PERMEABILITY

by

Kishan NAIKOTI* and Meenakshi VADITHYA

Department of Mathematics, University College of Science, Osmania University, Hyderabad, Andra Pradesh

Original scientific paper
DOI: 10.2298/TSCI111230104N

This paper deals with the problem of thermal radiation effects on magnetohydrodynamic flow and heat transfer in a channel with porous walls of different permeability. The equations governing the flow are coupled non-linear partial differential equations. By introducing the stream function, the governing partial differential equations are reduced to ordinary differential equations. The governing equations which are coupled and highly non-linear are first linearized by quasi-linearization technique and obtained numerical solution by using implicit finite difference scheme. The effects of various parameters, namely, Reynolds number, permeability parameter, Hartmann number, Prandtl number, and thermal radiation parameter, entering into the problem on the velocity field and temperature distribution are shown graphically.

Key words: *magnetohydrodynamic, thermal radiation, permeability parameter, finite difference method, Reynolds number, Hartmann number*

Introduction

The heating of rooms and buildings by the use of radiators is a familiar example of heat transfer by free convection. Heat losses from hot pipes, ovens *etc*., surrounded by cooler air, are at least in part, due to free convection. However, the mixed types of problems are very important and have many industrial and technological applications. The problem of radiation transfer in a vertical channel has been studied in recent times as a model for the re-entry problem. This is due to the significant role of thermal radiation in surface heat transfer when convection heat transfer is similar, particularly in free convection problems involving absorbing emitting fluids. Hossain and Takhar [1] analyzed the effect of radiation using the Rosseland diffusion approximation that leads to non-similar boundary layer equations governing the mixed convection flow of an optically dense viscous incompressible fluid past a heated vertical plate with a uniform free stream velocity and surface temperature. In the past years Ferdows, *et al.* [2] has studied the numerical approach on parameters of the thermal radiation interaction with plate with variable suction parameter.

Considerable attention has been given to the unsteady free-convection flow of viscous incompressible, electrically conducting fluid in the presence of applied magnetic field in connection with the theories of fluid motion in the liquid core of the earth, meteorological, and oceanographic applications. When the strength of applied magnetic field is very strong, one cannot neglect the effect of Hall currents. Due to the gyration and drift of charged particles the conductivity parallel to the electric field is reduced and the current is induced in the

* Corresponding author; e-mail: kishan_n@rediffmail.com

direction normal to both electric and magnetic fields. This phenomenon is known as the Hall effect. This effect can be taken into account within the range of magnetohydrodynamical approximation. Sato [3] has studied the effect of Hall currents on the steady hydro magnetic flow between two parallel plates. Sattar and Hossain [4] studied the unsteady hydro magnetic free convection flow with Hall current and mass transfer along an accelerated porous plate with time dependent temperature and concentration. The effect of Hall current on magnetohydrodynamic flow and heat transfer along a porous flat plate with mass transfer is studied by Sriramulu *et al.* [5].

The problem of magnetohydrodynamic flow and heat transfer through porous ducts has been analyzed by several authors like Terrill and Shreshtha [6], Alpher [7], Berman [8], Nigam and Singh [9] in the past few years. An extension of the above problem has been made here to magnetohydrodynamics for which both flow and heat transfer has been discussed. The effects of thermal radiation on magnetohydrodynamic flow and heat transfer through porous ducts has been analyzed by several authors like Bataller [10], Chamkha [11], Mahmoud [12], and Sattar and Kalim [13]. Recently, the magnetohydrodynamic heat and mass transfer of free convection flow near the lower stagnation point of an isothermal cylinder embedded in porous domain with the presence of radiation is studied by Uddin and Kumar [14].

In most of the earlier problems, in general, series solution have been taken to find the velocity functions where one is restricted to take only a finite number of terms which puts a limitation on the values of the parameter involved. In this particular paper, method of quasi-linearization, as discussed by Bellmann and Kalaba [15] has been used to find the velocity function and heat transfer. The beauty of this technique lies in that (1) it converges quadratically, (2) solution is valid for a large range of value of the parameters, and (3) the original basis equation can be used directly without much elaboration. Recently, Bhargava and Rani [16] have used the same technique and solved by using the Runge-Kutta method for the problem of magnetohydrodynamic flow and heat transfer in a channel with porous walls of different permeability.

The present investigation is to study the effects of thermal radiation on magnetohydrodynamic flow and heat transfer in a channel with porous walls of different permeability by using the quasi-linearization technique with the finite difference scheme. The C-programming is used to compute the numerical values of f, f', and θ for different values of the flow parameters.

Mathematical analysis

Consider a steady laminar and incompressible flow in a channel of width h, which is bounded by two porous walls of different permeability. A constant magnetic field is applied normal to the axis of the channel. The induced magnetic field has been neglected in the flow since the magnetic Reynolds number in small. Let u and v be the components of the velocity along Ox and Oy. Further define a non-dimensional variable:

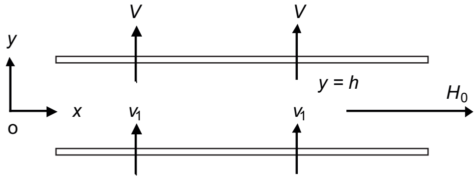

Figure 1. Schematic figure

$$\lambda = \frac{y}{h} \tag{1}$$

Let v be equal to v_1 at the wall $y = 0$ and V at the wall $y = h$. Without loss of generality, it is assumed that $|v| \geq |v_1|$.

The equation of continuity, momentum and energy becomes:

$$\frac{\partial u}{\partial x}+\frac{1}{h}\frac{\partial v}{\partial \lambda}=0 \tag{2}$$

$$u\frac{\partial u}{\partial x}+\frac{v}{h}\frac{\partial u}{\partial \lambda}=-\frac{1}{\rho}\frac{\partial p}{\partial x}+\frac{\mu}{\rho}\left(\frac{\partial^2 u}{\partial x^2}+\frac{1}{h^2}\frac{\partial^2 u}{\partial \lambda^2}\right)-\frac{{\mu_e}^2 H_0^2\sigma}{\rho}u-\left(\frac{\mu}{\kappa}\right)u \tag{3}$$

$$u\frac{\partial v}{\partial x}+\frac{v}{h}\frac{\partial v}{\partial \lambda}=-\frac{1}{\rho h}\frac{\partial p}{\partial \lambda}+\frac{\mu}{\rho}\left(\frac{\partial^2 v}{\partial x^2}+\frac{1}{h^2}\frac{\partial^2 v}{\partial \lambda^2}\right)-\left(\frac{\mu}{\kappa}\right)v \tag{4}$$

$$u\frac{\partial T}{\partial x}+v\frac{\partial T}{\partial y}=\frac{\kappa}{\rho C_p}\frac{\partial^2 T}{\partial y^2}+\frac{\mu}{\rho C_p}\left(\frac{\partial u}{\partial y}\right)^2+\frac{\sigma\mu_e^2 H_0^2}{\rho C_p}u^2-\left(\frac{1}{\rho C_p}\right)\left(\frac{\partial q_r}{\partial y}\right) \tag{5}$$

where ρ is the fluid density, p – the pressure, μ – the coefficient of viscosity, σ – the electric permeability, C_p – the specific heat at the constant pressure, and κ – the coefficient of thermal conductivity.

The boundary conditions are:

$$u(x,\lambda)=0,\quad v(x,\lambda)=v_1,\quad T=T_0 \quad \text{at} \quad \lambda=0 \tag{6}$$

$$u(x,\lambda)=0,\quad v(x,\lambda)=V,\quad T=T_1 \quad \text{at} \quad \lambda=1$$

We take the stream function for the flow, as Terrill and Shrestha [17]:

$$\psi(x,\lambda)=(hU-Vx)f(\lambda) \tag{7}$$

where U is the entrance velocity.

Accordingly:

$$u(x,\lambda)=\left(U-\frac{Vx}{h}\right)f'(\lambda) \quad \text{and} \quad v(x,\lambda)=Vf(\lambda) \tag{8}$$

where prime denotes differentiation with respect to λ.

Substitution of eq. (8) in eqs. (3) and (4) yields:

$$-\frac{1}{\rho}\frac{\partial p}{\partial x}=\left(U-\frac{Vx}{h}\right)\left(-\frac{V}{h}f'^2+\frac{V}{h}ff''-\frac{\mu}{\rho h^2}f'''-\frac{\mu_e^2 H_0^2\sigma}{\rho}f'\right) \tag{9}$$

$$-\frac{1}{\rho}\frac{\partial p}{\partial \lambda}=V^2 ff'-\frac{\mu V}{\rho h}f'' \tag{10}$$

Eliminating p from (9) and (10), we finally get:

$$\mathrm{Re}(f'f''-ff''')+f^{iv}+(S^2+K)f''=0 \tag{11}$$

where $\mathrm{Re}=\rho Vh/\mu$ is the Reynolds number, $S^2=\mu_e H_0 h(\sigma/\mu)^{-1/2}$ is the Hartmann number, and $K=(\rho h^2/k)$ is the permeability parameter.

Equation (5) together with eq. (8) suggest that the form of temperature distribution can be taken as:

$$T = T_0 + \frac{\nu V}{hC_p}\left[\varphi(\lambda) + \left(\frac{U}{V} - \frac{x}{h}\right)^2 \psi(\lambda)\right] \tag{12}$$

Substitution of eq. (12) in eq. (5), and equating the coefficient of $(U/V) - (x/h)$ on both sides of the equation thus obtained, we have:

$$\frac{1}{\text{Re}\,\text{Pr}}(1+F)\varphi'' - f\varphi' = 0 \tag{13}$$

$$\frac{1}{\text{Re}\,\text{Pr}}(1+F)\psi'' - f\psi' + 2f\psi + f''^2 + \text{S}^2 f'^2 = 0 \tag{14}$$

where $\text{Pr} = \mu C_p/k$ is the Prandtl number.

$$\frac{\partial q_r}{\partial y} = \frac{-16\sigma^* T_\infty^3}{3k}\frac{\partial^2 T}{\partial y^2}, \quad \text{and} \quad F = \frac{-16\sigma^* T_\infty^3}{3k^2}$$

is the radiation parameter.

Also, in the dimensionless form, the temperature, eq. (12), can be expressed as:

$$\theta = \frac{T - T_0}{T_1 - T_0} = \text{Ec}(\varphi + \chi^2 \psi) \tag{15}$$

where $\text{Ec} = \nu V/[(T_1 - T_0)hC_p]$ is the Eckert number and $\chi = (U/V) - (x/h)$ is the dimensionless distances. The boundary conditions (6) can be written as:

$$f'(1) = 0, \quad f(1) = \frac{v_1}{V} = \alpha, \quad \varphi = \psi = 0 \quad \text{at} \quad \lambda = 0$$

$$f^1(1) = 0, \quad f(1) = 1, \quad \varphi = \frac{1}{\text{Ec}} = \omega, \quad \psi = 0 \quad \text{at} \quad \lambda = 1 \tag{16}$$

Method of solution

The flow, eq. (11), is decoupled from the energy eqs. (13) and (14), and need to be solved before the latter can be solved. The flow constitutes a non-linear boundary value problem. In the absence of analytical solution of a problem, a numerical solution is indeed an obvious and natural choice. The eq. (11) may be viewed as a prototype for numerous other situations which are similarly characterized by a boundary value problem having a fourth order differential equation with an asymptotic boundary conditions. Therefore, its numerical solution merits attention from a practical point of view. A quasi-linearization technique, Bellmann and Kalaba [15], is applied to replace the non-linear terms at a linear stage, with the corrections incorporated in subsequent iterative steps until convergence. The quasi-linearized form of eq. (11) is:

$$f^{iv} - \text{Re}\, f'''F + (\text{Re}\,F' + S^2 + K)f'' + \text{Re}\, f'F'' - \text{Re}\, fF''' = \text{Re}\,F'F'' - \text{Re}\,FF''' \tag{17}$$

where F represents the n^{th} approximation to the solution, and f represents the $(n+1)^{\text{th}}$ approximation to the solution.

$$f^{iv} - A1[i]f''' + A2[i]f'' + A3[i]f' - A4[i]f = D[i] \tag{18}$$

where $A1[i] = \mathrm{Re}F$, $A2[i] = \mathrm{Re}F + \mathrm{S}^2$, $A3[i] = \mathrm{Re}F''$, $A4[i] = \mathrm{Re}F'''$, $D[i] = \mathrm{Re}F''F' - \mathrm{Re}FF'''$.

Using implicit finite difference method to eq. (18) we get:

$$B1[i]f[i+2] + B2[i]f[i+1] + B3[i]f[i] + B4[i]f[i-1] + B5[i]f[i-2] = E[i] \tag{19}$$

where

$$B1[i] = 2 - \Delta\lambda A1[i], \quad B2[i] = 2(\Delta\lambda)A1[i] + 2(\Delta\lambda)^2 A2[i] + 2(\Delta\lambda)^3 A3[i] - 8,$$

$$B3[i] = 12 - 4(\Delta\lambda)^2 A2[i] - 2(\Delta\lambda)^3 A3[i], \quad B4[i] = 2(\Delta\lambda)^2 A2[i] - 2(\Delta\lambda)\ A1[i] - 8,$$

$$B5[i] = 2 + (\Delta\lambda)A1[i], \quad E[i] = 2(\Delta\lambda)^4 D[i]$$

With the implicit finite difference method the eqs. (13)-(14) are reduced to:

$$C1[i]\varphi[i+1] - 4\varphi[i] + C2[i]\varphi[i-1] = 0$$

$$D1[i]\psi[i+1] + D2[i]\psi[i] + D3[i]\psi[i-1] + E1[i] = 0 \tag{21}$$

where

$$C1[i] = 2(1+F) - \Delta\lambda\mathrm{PrRe}, \quad C2[i] = 2(1+F) + \Delta\lambda\mathrm{PrRe},$$

$$D1[i] = 2(1+F) - \Delta\lambda\mathrm{RePr}F[i], \quad D2[i] = 4\left\{\mathrm{RePr}(\Delta\lambda)^2 F_1[i]\right\} - 4(1+F),$$

$$D3[i] = 2(1+F) + \Delta\lambda\mathrm{RePr}F[i], \quad E1[i] = 2\left\{(\Delta\lambda)^2 \mathrm{RePr}F_2^2[i]\right\} + 2\left\{(\Delta\lambda)^2 \mathrm{RePrS}^2 F_1^2[i]\right\}$$

Here, $\Delta\lambda$ represents the mesh size. An iteration scheme is used to solve the quasi-linearized system of difference eqs. (19)-(21). The resulting black tri-diagonal system was solved by using Thomas algorithm. The resulting system of equations has to be solved in the finite domain $0 < \lambda < 1$. Here the step size has taken $\Delta\lambda = 0.05$. The obtained numerical values φ and ψ are to be substituted in eq. (15), to get the solution for temperature θ. The iterations are continued till the convergence within prescribed accuracy *i. e.*, $|f - F| < 10^{-5}$.

Results and discussions

The values functions f, f', ψ, φ, and θ have been computed for different values of Reynolds number, Hartmann number, Prandtl number, Eckert number, permeability parameter, radiation parameter, and ω. The numerical values of *f and f'* have been calculated for Re and S^2. The temperature functions ψ, φ, and θ have been calculated for Ec = 2.0, $\omega = 1.0$, and Pr = 0.2, 0.4, 2.0. Here, positive Reynolds number means injection through the wall at $\lambda = 0$ and suction at $\lambda = 1$ while negative Reynolds number represents the injection at the upper wall and suction at the lower wall.

Figure 2 shows the variation of velocity profiles $f(\lambda)$ for different values of Reynolds number when $\mathrm{S}^2 = 0.2$. It is observed that the value of $f(\lambda)$ decreases as Reynolds number increases due to increase in the inertia. The variation of velocity profile $f(\lambda)$ is shown in fig. 3, for different Hartmann number values for Re = 0.4. It is observed that velocity profiles $f(\lambda)$ decreases as Hartmann number increases. The application of a transverse magnetic field to an electrically conducting fluid gives rise to a resistive force called Lorentz force. This force has the tendency to slow down the motion of the fluid. Figures 4(a) and (b) shows that the variation of velocity profiles $f(\lambda)$ for different values of permeability parameter for fixed values of $S^2 = 0.2$ and Re = 0.4 and –13.88. It is observed that the value of $f(\lambda)$ decreases as the permeability parameter increases in both the cases. It is also observed that the effect of permeability parameter is more in case of Re = 0.4 when compared with the Re = –13.88.

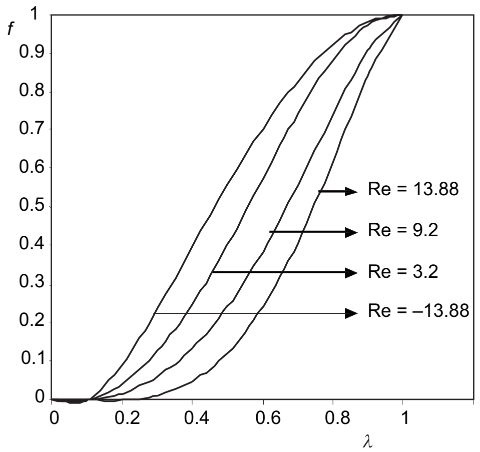

Figure 2. Variation of velocity profiles $f(\lambda)$ for different values of Re and S^2 = 0.2

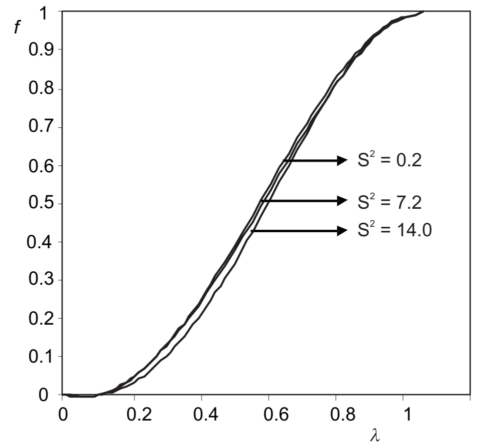

Figure 3. Variation of velocity profiles $f(\lambda)$ for Re = 0.4 and different S^2

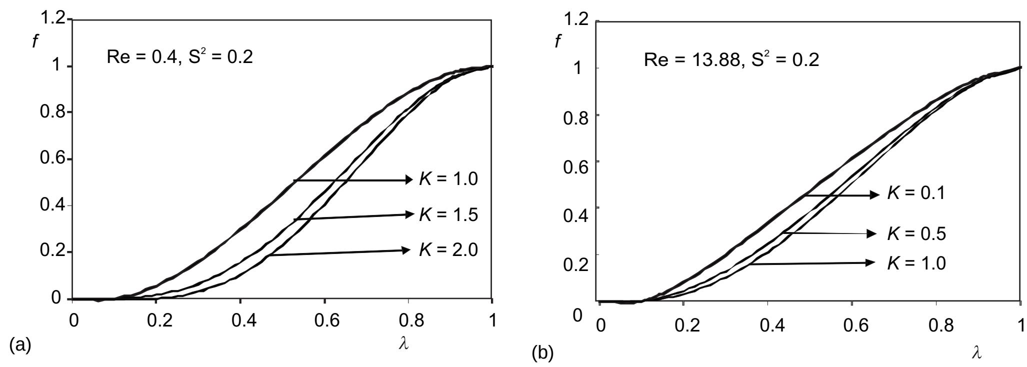

Figure 4. (a) Variation of velocity profiles $f(\lambda)$ for different values of *K*; (b) variation of velocity profiles $f(\lambda)$ for different values of *K*

From fig. 5, it is clear that as Reynolds number decreases the velocity profiles $f'(\lambda)$ increases near the lower wall $\lambda = 0$,while $f'(\lambda)$ increases as Reynolds number increases near the upper wall $\lambda = 1$ for different Re and $S^2 = 0.2$ due to inertia. It is also noticed that the maxima is shifting towards the upper wall $\lambda = 1$. From fig. 6, it is observed that the velocity profiles $f'(\lambda)$ decreases with the increase of Hartmann number near the lower wall ($\lambda = 0$), whereas the velocity increases near the upper wall ($\lambda = 1$) with the increase of Hartmann number. It is clear from the figure that the maximum $f'(\lambda)$ value is shifting towards the upper wall. From figs. 7(a) and (b), it can be seen that the effect of permeability parameter *K* on velocity profiles $f'(\lambda)$ for different values of Reynolds number *i. e.*, Re = –13.88 and Re = 9.2 with fixed value of $S^2 = 0.2$. It is observed that $f'(\lambda)$ decreases near the lower wall $\lambda = 0$, while it increases as permeability factor increases on the other side of the wall. It is noticed that the effect of permeability factor is more when Re = –13.88 comparing with Re = 9.2.

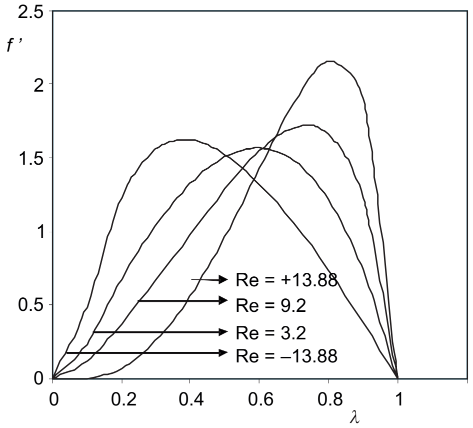

Figure 5. Variation of $f'(\lambda)$ for different values of Re and $S^2 = 0.2$

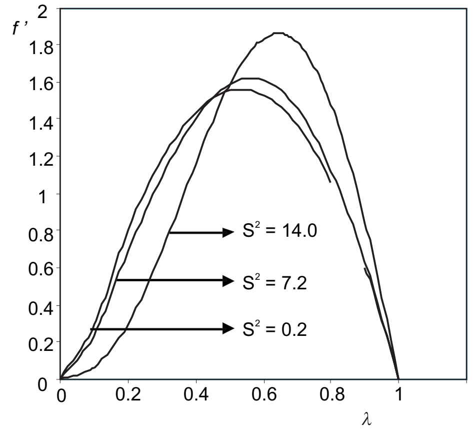

Figure 6. Variation of $f'(\lambda)$ for different values of S^2 and Re = 0.4

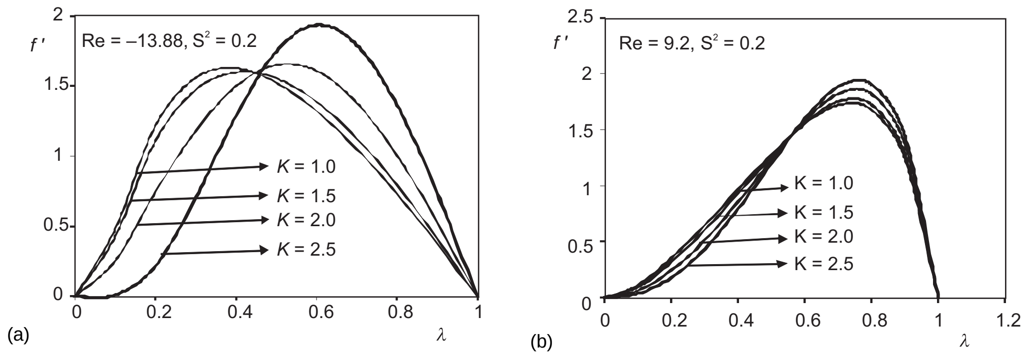

Figure 7. (a) Variation of velocity profiles $f'(\lambda)$ for different values of *K*; (b) variation of velocity profiles $f'(\lambda)$ for different values of *K*

The temperature variation for different Reynolds number and Prandtl number values are shown in fig. 8. The temperature distribution got a convex shape downwards for negative Reynolds number, while it has a reverse trend for positive values of Reynolds number. The temperature profiles decreases as Reynolds number decreases. The temperature profiles decreases as Prandtl number increases for the positive Reynolds number where the temperature profiles increases with the increase of Prandtl number in negative Reynolds number. The temperature distribution increases as Hartmann number increases is noticed from fig. 9. The Prandtl number defines the ratio of momentum diffusivity to thermal diffusivity. The reasons the smaller values of Prandtl number are equivalent to increase in the thermal conductivities, and therefore heat is able to diffuse away from the heated surface more rapidly than for higher values of Prandtl number. Hence, in the case of smaller Prandtl number as the boundary layer is thicker and the rate of heat transfer is reduced.

Figure 10 shows that the variation of temperature profiles $\theta(\lambda)$ for different values of radiation parameter. It can be observed from fig. 10(a) as the values of radiation parameter increases the temperature profiles $\theta(\lambda)$ decreases when Re = 13.88, $S^2 = 0.2$, and Pr = 0.4. Figure 10(b) shows that the temperature profiles $\theta(\lambda)$ for the different values of radiation parameter when Re = 0.4, $S^2 = 25.0$, Pr = 0.2 are fixed, it is observed that the temperature profiles decreases as radiation parameter increases. Decrease in thermal radiation parameter (*i. e.* incre-

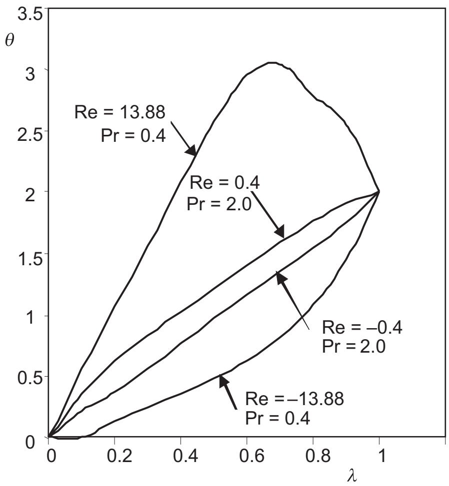

Figure 8. Temperature variation for different Reynolds and Prandtl number

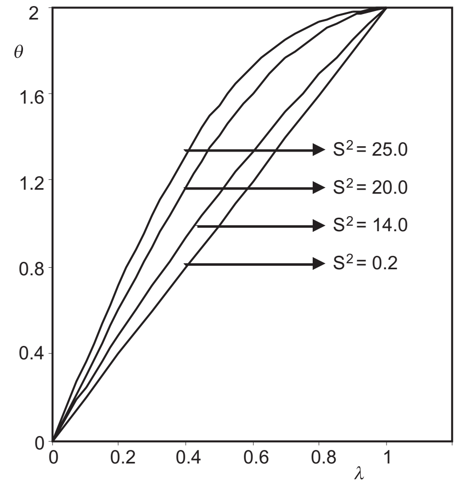

Figure 9. Temperature variation for different values of S^2 and Re = 0.4, and Pr = 0.2

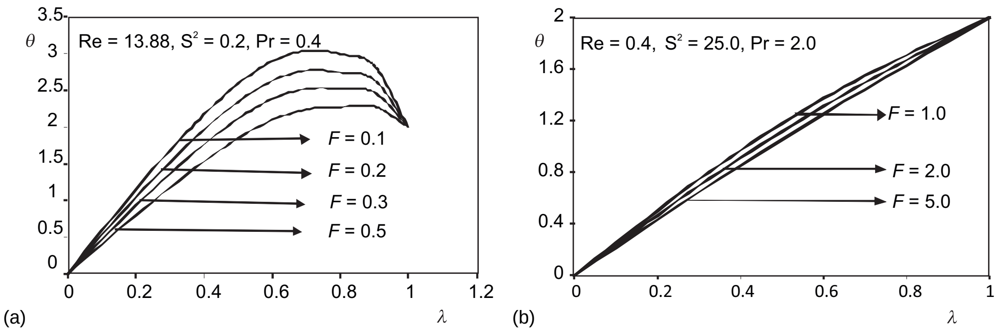

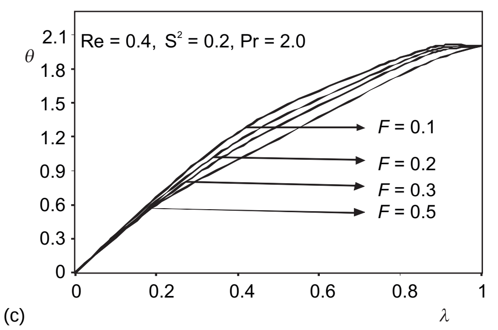

Figure 10. Variation of temperature profiles $\theta(\lambda)$ for different values of the radiation parameter

ase in radiation effects) produces the significant in the thermal state of fluid causing the temperature to increase. This increase in the fluid temperature induces through the effect of thermal buoyancy more flow in the boundary layer causing the velocity of the fluid there to increase. This may be attributed to the fact that the increase of the values of radiation parameter implies less interaction of radiation with the momentum boundary layer and thermal boundary layer. When $F \to \infty$ there is no radiation effect. Figure 10(c) shows that the temperature profiles $\theta(\lambda)$ when Re = 0.4, S^2 = 0.2, and Pr = 2.0. It is noticed that the temperature profiles decreases as radiation parameter increases. It is also evident from the above three figures, the effect of radiation parameter is less when Hartmann number $S^2 = 25.0$ compared with $S^2 = 0.2$.

Conclusions

In the paper the effects of the thermal radiation on steady MHD flow and heat transfer in a channel with porous walls of different permeability is studied. The governing equations are non-dimensionalized and linearized by using quasi-linearization technique. They are solved by using the implicit finite difference method. From the above mentioned discussion, the following conclusions can be drawn.

- An increase in the Hartmann number the velocity profile f' decreases near the lower wall ($\lambda = 0$), the reverse phenomena is observed near the upper wall ($\lambda = 1$). The temperature profiles increases with the increase in Hartmann number.
- The effect of radiation parameter F is to reduce the temperature profiles. It is observed that the radiation parameter effect is significantly more for higher values of Reynolds number (Re = 13.88).
- An increase in the Reynolds number reduce the velocity profiles f' near the lower wall ($\lambda = 0$), increase near the upper wall ($\lambda = 1$).
- The effect of permeability parameter on velocity profiles f' is to decreases near the lower wall $\lambda = 0$, the reverse phenomena is observed near the upper wall ($\lambda = 1$). The effect of permeability parameter is more significantly when Re = –13.88 compare with other cases.

Nomenclature

C_p – specific heat at constant pressure, [$Jkg^{-1}K^{-1}$]
Ec – Eckert number
F – radiation parameter
f – longitudinal velocity
f' – transverse velocity
H_0 – magnetic field
K – permeability parameter
p – pressure, [mmHg]
Pr – Prandtl number
q_r – radiative heat flux
Re – Reynolds number
S^2 – Hartmann number
T – dimensionless temperature, [K]
T_0, T_1 – wall temperature at walls $y = 0$, and at $y = h$, respectively, [K]
u, v – velocity components along x- and y-direction, respectively, [ms^{-1}]
v_1, V – velocity components at walls $y = 0$, and at $y = h$, respectively, [ms^{-1}]
x – Cartesian co-ordinate along the plate
y – Cartesian co-ordinate normal to the plate

Greek symbols

α – constant
θ – dimensionless temperature
κ – the thermal conductivity, [$Wm^{-1}K^{-1}$]
μ – coefficient of viscosity, [$kgm^{-1}s^{-1}$]
μ_e – effective viscosity
ν – kinematic viscosity, [m^2s^{-1}]
ρ – density of the fluid, [kgm^{-3}]
σ – electric permeability
σ^* – Stefan-Boltzman constant ($5.6703 \cdot 10^{-8}$), [$Wm^{-2}K^{-4}$]
φ – dimensional velocity function
ψ – dimensional stream function
ω – constants

References

[1] Hossain, M. A., Takhar, H. S, Radiation Effect on Mixed Convection along a Vertical Plate with Uniform Surface Temperature, *Heat and Mass Transfer, 31* (1996), 4, pp. 243-248
[2] Ferdows, M., *et al.,* Numerical Approach on Parameters of the Thermal Radiation Interaction with Convection in a Boundary Layer Flow at a Vertical Plate with Variable Suction, *Thammasat Int. Jour. Sci. Tech, 9* (2004), 3, pp. 19-28
[3] Sato, H, The Hall Effect in the Viscous Flow of Ionized Gas between Parallel Plates under Transverse Magnetic Field, *Journal of Physics Society of Japan, 16* (1961), pp 1427-1433

[4] Sattar, M. A., Hossain, M. M., Unsteady Hydro Magnetic Free Convection Flow with the Hall Current and Mass Transfer along an Accelerated Porous Plate with Time Dependent Temperature and Concentration, *Can. J. Phys*., 70 (1992) 5, pp. 369-374
[5] Sriramulu, A., *et al.,* Magnetohydrodynamic Flow with Suction or Injection at the Forward Stagnation Point of an Infinite Plane Wall, *Far East J. Appl. Math.,* 13 (2003), 1, pp. 1-11
[6] Terrill, R. M., Shrestha, G. M., Laminar Flow in a Uniformly Porous Channel with an Applied Transverse Magnetic Field, *Appl. Sci. Res., 12* (1965), 3, pp. 203-211
[7] Alpher, R. A., Heat Transfer in Magnetohydrodynamic Flow between Parallel Plates*, Int. J. Heat Mass Transfer*, *13* (1961), 2, pp. 108-112
[8] Berman, A. S., Laminar Flow in Channels with Porous Walls, *J. Appl. Phys., 24* (1953), 9, pp. 1232-1235
[9] Nigam, S. D., Singh, S. N., Heat Transfer by Laminar Flow between Parallel Plates under the Action of Transverse Magnetic Field, *Q. J. Mech. Appl. Math., 13* (1960), 1, pp. 85-97
[10] Bataller, C. R., Magnetohydrodynamic Boundary Layer Flow and Heat Transfer of a Non-Newtonian Power-Law Fluid past a Moving Plate with Thermal Radiation, *Il Nuovo Cimento B, 121* (2006), 9, pp 951-964
[11] Chamkha, A. J., Thermal Radiation and Buoyancy Effects on Hydromagnetic Flow over an Accelerating Permeable Surface with Heat Source or Sink, *Int. Journal of Engineering Science 38(15)* (2000), 10, pp. 1699-1712
[12] Mahmoud, M. A. A., Thermal Radiation Effects on Magnetohydrodynamic Flow of a Micropolar Fluid over a Stretching Surface with Variable Thermal Conductivity, *Physica A., 375* (2007), 2, pp. 401-410
[13] Sattar, M. A., Kalim, H., Unsteady Free Convection Interaction with Thermal Radiation in a Boundary Later Flow past a Vertical Porous Plate, *Journal of Mathematics and Physical Sciences,* 30 (1996), 1, pp. 25-37
[14] Uddin, Z., Kumar, M., Magnetohydrodynamic Heat and Mass Transfer of a Free Convection Flow near the Lower Stagnation Point of an Isothermal Cylinder Imbedded in Porous Domain with the Presence of Radiation, *Jordan Journal of Mechanical and Industrial Engineering IB, 5* (2011), 2, pp. 133-138
[15] Bellmann, R., Kalaba, R., *Quasi-Linearization and Non-Linear Boundary Value Problems,* American Elsevier, New York, USA, 1965
[16] Bhargava, R., Rani, M., Magnetohydrodynamic Flow and Heat Transfer in a Channel with Porous Walls of Different Permeability, *Indian J. Pure and Appl. Maths*, *15* (1984), 4, pp. 397-408
[17] Terrill, R. M., Shrestha, G. M., Laminar Flow in a Porous Channel of Different Permeability, *Appl. Sci. Res., 11* (1964), 1, pp. 134-144

Paper submitted: August 26, 2011
Paper revised: May 30, 2012
Paper accepted: May 30, 2012